THE JOURNAL OF BIOLOGICAL CHEMISTRY
Vol. 280, No. 18, Issue of May 6, pp. 17863–17872, 2005

*Printed in U.S.A.*

# Structural and Functional Characterization of Transmembrane Segment IV of the NHE1 Isoform of the $Na^+/H^+$ Exchanger*

Received for publication, August 20, 2004, and in revised form, January 14, 2005
Published, JBC Papers in Press, January 26, 2005, DOI 10.1074/jbc. M409608200

**Emily R. Slepkov‡§, Jan K. Rainey¶‖, Xiuju Li‡**, Yongsheng Liu‡, Florence J. Cheng‡, Darrin A. Lindhout‡‡§§, Brian D. Sykes¶‡‡¶¶, and Larry Fliegel‡‖‖**

*From the ‡Membrane Protein Research Group, Department of Biochemistry, ‡‡Canadian Institutes of Health Research Group in Protein Structure and Function, and ¶Protein Engineering Network of Centers of Excellence, University of Alberta, Edmonton, Alberta T6G 2H7, Canada*

**The $Na^+/H^+$ exchanger isoform 1 is a ubiquitously expressed integral membrane protein that regulates intracellular pH in mammals. We characterized the structural and functional aspects of the critical transmembrane (TM) segment IV. Each residue was mutated to cysteine in cysteine-less NHE1. TM IV was exquisitely sensitive to mutation with 10 of 23 mutations causing greatly reduced expression and/or activity. The $Phe^{161} \rightarrow$ Cys mutant was inhibited by treatment with the water-soluble sulfhydryl-reactive compounds [2-(trimethylammonium)ethyl]methanethiosulfonate and [2-sulfonatoethyl]methanethiosulfonate, suggesting it is a pore-lining residue. The structure of purified TM IV peptide was determined using high resolution NMR in a $CD_3OH$:$CDCl_3$:$H_2O$ mixture and in $Me_2SO$. In $CD_3OH$:$CDCl_3$:$H_2O$, TM IV was structured but not as a canonical $\alpha$-helix. Residues $Asp^{159}$–$Leu^{162}$ were a series of $\beta$-turns; residues $Leu^{165}$–$Pro^{168}$ showed an extended structure, and residues $Ile^{169}$–$Phe^{176}$ were helical in character. These three structured regions rotated quite freely with respect to the others. In $Me_2SO$, the structure was much less defined. Our results demonstrate that TM IV is an unusually structured transmembrane segment that is exquisitely sensitive to mutagenesis and that $Phe^{161}$ is a pore-lining residue.**

The mammalian $Na^+/H^+$ exchanger isoform 1 (NHE1)[1] is a ubiquitously expressed integral membrane protein that mediates the removal of one intracellular proton in exchange for one extracellular sodium ion (1). NHE1 thereby protects cells from intracellular acidification (2, 3); and stimulation of its activity promotes cell growth and differentiation (2) and regulates sodium fluxes and cell volume after osmotic shrinkage (2, 3). The $Na^+/H^+$ exchanger also plays an important role in the damage that occurs to the human myocardium during ischemia and reperfusion, and it has been shown that inhibition of the exchanger has beneficial effects on the myocardium under these conditions (4). Amiloride and its derivatives are inhibitors of the NHE1 isoform of the $Na^+/H^+$ exchanger, and a new generation of $Na^+/H^+$ exchanger inhibitors is being developed for clinical treatment of heart disease (5).

Although the activity of NHE1 has been extensively examined in many tissues, only recently is information starting to be elucidated on how this antiporter actually binds and transports $Na^+$ ions and protons. NHE1 is composed of two domains as follows: an N-terminal membrane domain of ~500 amino acids and a C-terminal regulatory domain of about 315 amino acids (1, 4) (Fig. 1). The N-terminal membrane domain is responsible for ion movement, and it is reported to have 12 transmembrane (TM) segments and 3 membrane-associated segments (6). Transmembrane segment four (TM IV; residues 155–177) has been implicated in the ion transport and inhibitor binding properties of NHE1 (7–9). The sequence of human TM IV of NHE1 is $^{155}$FLQSDVFFLFLLPPIILDAGYFL$^{177}$. The underlined residues have been shown to affect $Na^+$ affinity or the inhibitor resistance of mammalian NHE1 (7–9). Recently, we have shown that prolines 167 and 168 are critical forNHE1 function, targeting, and expression (10). These data provide a strong case for the importance of many amino acid residues of TM IV in the ion binding, structure, and transport properties of NHE1.

In this communication, we examine both structural and functional aspects of TM IV of the NHE1 isoform of the $Na^+/H^+$ exchanger. We use cysteine-scanning mutagenesis to characterize which amino acids are important in function and are

* This work was supported in part by funds from the Canadian Institutes of Health Research (to L. F.) and from the Canadian Institutes of Health Research and Protein Engineering Network of Centers of Excellence (to B. D. S.). The costs of publication of this article were defrayed in part by the payment of page charges. This article must therefore be hereby marked "*advertisement*" in accordance with 18 U.S.C. Section 1734 solely to indicate this fact.

*The atomic coordinates and structure factors (code 1Y4E) have been deposited in the Protein Data Bank, Research Collaboratory for Structural Bioinformatics, Rutgers University, New Brunswick, NJ (http://www.rcsb.org/).*

§ Supported by studentship awards from the Alberta Heritage Foundation for Medical Research and the Heart and Stroke Foundation of Canada.

‖ Supported by postdoctoral fellowships from the Natural Sciences and Engineering Research Council of Canada and the Alberta Heritage Foundation for Medical Research.

** Supported in part by Canadian Institutes of Health Research Strategic Training Initiative in Membrane Proteins and Cardiovascular Disease.

§§ Supported by an Alberta Heritage Foundation for Medical Research studentship.

¶¶ Recipient of support as a Canada Research Chair in Structural Biology.

‖‖ Supported by a scientist award from the Alberta Heritage Foundation for Medical Research. To whom correspondence should be addressed: Dept. of Biochemistry, 347 Medical Science Bldg., University of Alberta, Edmonton, Alberta T6G 2H7, Canada. Tel.: 780-492-1848; Fax: 780-492-0886; E-mail: lfliegel@ualberta.ca.

[1] The abbreviations used are: NHE1–8, $Na^+/H^+$ exchanger isoforms 1–8; cNHE1, cysteine-less NHE1; $Me_2SO$, dimethyl sulfoxide; DSS, sodium 2,2-dimethyl-2-silapentane-5-sulfonate; HA, hemagglutinin; HNHA, $^{15}$N-edited $^1H^N$-$^1H^\alpha$ correlation spectroscopy; HSQC, heteronuclear single quantum coherence spectroscopy; MALDI-MS, matrix assisted laser-desorption ionization mass spectrometry; MTSES ([2-sulfonatoethyl]methanethiosulfonate); MTSET, [2-(trimethylammonium)ethyl]methanethiosulfonate; NOE, nuclear Overhauser effect; NOESY, nuclear Overhauser enhancement spectroscopy; r.m.s.d., root-mean-square deviation; TM, transmembrane segment; TOCSY, total correlation spectroscopy; HPLC, high pressure liquid chromatography.

likely pore-lining residues of TM IV. To study the structure of TM IV, the segment was expressed and purified, and we compared its structure in two different membrane mimetic solvent conditions. This provides insight into structured regions, in our case, without fixing the segment as a whole into a single conformation. The use of solution conditions having a low dielectric constant to mimic a membrane environment has become quite common for structural studies of transmembrane proteins or peptides and has provided structures of isolated protein segments consistent with their structures in the full protein (11–13). Our study demonstrates that whereas TM IV is structured, only a 4–6-residue stretch of the segment is helical. In addition, we identify $Phe^{161}$ as a pore-lining residue in NHE1.

## EXPERIMENTAL PROCEDURES

*Materials*—$^{15}N$-Labeled ammonium sulfate and all deuterated NMR solvents were from Cambridge Isotope Laboratories (Andover, MA). Pwo DNA polymerase was from Roche Applied Science. Lipofectamine™ 2000 Reagent was from Invitrogen. MTSET and MTSES were from Toronto Research Chemicals (Toronto, Ontario, Canada).

*Site-directed Mutagenesis*—Mutations in TM IV were made to an expression plasmid containing a hemagglutinin (HA)-tagged human NHE1 isoform of the $Na^+/H^+$ exchanger. The plasmid pYN4-C contains the cDNA of the entire coding of NHE1 with all 10 native cysteine residues mutated to serine as described earlier (10). Each residue of TM IV was individually mutated to cysteine using the cysteine-less pYN4-C as a template. Site-directed mutagenesis was performed using amplification with Pwo DNA polymerase followed by use of the Stratagene (La Jolla, CA) QuikChange™ site-directed mutagenesis kit as recommended by the manufacturer. Mutations were designed to create a new restriction enzyme site for use in screening transformants. DNA sequencing confirmed the accuracy of the mutations.

*Cell Culture and Stable Transfection*—AP-1 cells were used to examine $Na^+/H^+$ exchanger expression and activity. These cells lack an endogenous $Na^+/H^+$ exchanger. Stable cell lines were made of all mutants by transfection with Lipofectamine™ 2000 Reagent according to the manufacturer's protocol as described earlier (10). Transfected cells were selected using 800 $\mu$g/ml geneticin (G418), and stable cell lines for experiments were regularly re-established from frozen stocks at passage numbers between 5 and 15.

*SDS-PAGE and Immunoblotting*—To confirm NHE1 expression immunoblot, analysis was used on samples from total cell lysates of AP-1 cells. Cell lysates were made as described earlier (10). For Western blot analysis, equal amounts of each sample (100 $\mu$g total protein) were resolved on 10% SDS-polyacrylamide gels. The gel was transferred onto a nitrocellulose membrane and immunostained using anti-HA monoclonal antibody (Roche Applied Science) and peroxidase-conjugated goat anti-mouse antibody (Bio/Can, Mississauga, Ontario, Canada). The enhanced chemiluminescence Western blotting and detection system (Amersham Biosciences) was used to visualize immunoreactive proteins. Densitometric analysis of x-ray films was carried out using NIH Image 1.63 software (National Institutes of Health, Bethesda).

*Cell Surface Expression*—Cell surface expression was measured essentially as described earlier (10). Briefly, cells were labeled with Sulfo-NHS-SS-Biotin (Pierce), and immobilized streptavidin resin was used to remove cell surface-labeled $Na^+/H^+$ exchanger. Equivalent amounts of the total and unbound proteins were analyzed by SDS-PAGE, and Western blotting was as described above. The relative amount of NHE1 on the cell surface was calculated by comparing both the 110- and the 95-kDa species of NHE1 in Western blots of the total and unbound fractions. Results are shown as mean ± S.E. with statistical significance determined by a Mann-Whitney *U* test.

*$Na^+/H^+$ Exchange Activity and Sulfhydryl-reactive Reagent Inhibition*—$Na^+/H^+$ exchange activity was measured using a PTI Deltascan spectrofluorometer or a Schimadzu RF 5000 spectrofluorometer. The initial rate of $Na^+$-induced recovery of cytosolic pH ($pH_i$) was measured after acute acid load using 2′,7-bis(2-carboxyethyl)-5 (6) carboxyfluorescein-AM (Molecular Probes Inc., Eugene, OR). Ammonium chloride (50 mM for 3 min) was used to transiently induce an acid load, and the recovery in the presence of 135 mM NaCl was measured as described previously (10). There were no differences in buffering capacities of stable cell lines as indicated by the degree of acidification induced by ammonium chloride. Results are shown as mean ± S.E., and statistical significance was determined using a Mann-Whitney *U* test.

To test the effect of MTSET and MTSES on activity of the NHE1 mutants, we used the standard $Na^+/H^+$ exchanger assay with ammonium chloride-induced acidification of the cells. In this case cells were acidified two times as described above. After a first control acidification and recovery, either MTSET or MTSES was added to a final concentration of 10 mM for 10 min in $Na^+$-free buffer. The cells were subsequently washed three times in $Na^+$-free buffer prior to the second ammonium chloride-induced acidification and recovery. To calculate residual activity, Equation 1 was used,

$$\% \text{ residual activity} = \frac{\text{pH change after (reagent)}}{\text{pH change without (reagent)}} \times 100\% \quad \text{(Eq. 1)}$$

*Production and Purification of TM IV*—We produced TM IV as a fusion protein with the immunoglobulin binding domain of streptococcal protein G (GB1 domain). DNA encoding the residues of human NHE1 amino acids 155–180 ($^{155}$FLQSDVFFLFLLPPIILDAGYFLPLR-$^{180}$) was synthesized synthetically in the core facility of the Department of Biochemistry. Two self-annealing primers were designed to flank the protein sequence with Met residues and to change the codon preference to that favored in *Escherichia coli*. The primers were 5′-CTAGCATGTT TCTGCAGAGCGATGTGTTTTTTCTGTTTCTGCTGCCGCCGATTAT-TCTGGATGCGGGCTATTTTCTGCCGCTGCGCATGCCCGGGC-3′ and 5′-TCGAGCCCGGGCATGCGCAGCGGCAGAAAATAGCCCGCA-TCCAGAATAATCGGCGGCAGCAGAAACAGAAAAAACACATCGCT-CTGCAGAAACATG-3′. The primers were designed to have overhanging "sticky" NheI and XhoI ends so as to insert into the GEV-1 vector (14, 15). The annealed primers were ligated into the cut vector and transformed in *E. coli* XL1Blue and then later transformed into *E. coli* (BL21 DE3 pLysS) for protein production. The correct clones were verified by restriction enzyme digests and DNA sequencing. Cultures were induced with isopropyl 1-thio-$\beta$-D-galactopyranoside and treated to release the soluble protein as described earlier (14). For routine production of the protein, cultures were started from a single colony and grown in logarithmic stages until 2.0 liters. At $A_{600}$ of 0.8, cultures were induced with 1 mM isopropyl 1-thio-$\beta$-D-galactopyranoside for 5 h at 37 °C. Bacterial pellets were resuspended in 40 ml of 1× phosphate-buffered saline with 1% Triton X-100. The fusion protein was constructed such that a $His_6$ tag flanked the C-terminal Met. This was used for purification of the protein via nickel-nitrilotriacetic acid affinity chromatography as described by the manufacturer (Qiagen). The fusion protein was eluted from the column using 1 M imidazole. After purification, the eluted proteins concentrated using an Amicon concentrator and resuspended in 150 mM NaCl, 50 mM $Na_2HPO_4$. They were then desalted by using a Sephadex G-25 column in 10 mM $NH_4HCO_3$, pH 8.0, and then were lyophilized to dryness. To cleave the transmembrane segment IV free of GB1, standard techniques were employed. Briefly, a given purified batch of fusion peptide was lyophilized twice out of 0.05% (v/v) trifluoroacetic acid (trifluoroacetic acid; 99%, Aldrich) in water, dissolved to ~2 mg/ml in 50% (v/v) trifluoroacetic acid in water with excess cyanogen bromide (97%, Aldrich), and allowed to react in darkness for ~16 h at room temperature. The reaction mixture was quenched with an equal volume of deionized water and subsequently lyophilized. Reverse-phase HPLC was used to separate the various peptide products of the cleavage, and fractions containing the TM IV segment were pooled and lyophilized at least twice prior to use. The correct fragment identity was determined by MALDI mass spectrometry.

Preliminary experiments produced unlabeled TM IV. Later experiments produced labeled TM IV for more detailed characterization of the peptide structure. For these experiments, *E. coli* cells were grown in a minimal medium containing 87 mM $NaH_2PO_4$, 34 mM $K_2HPO_4$, 4 mM $MgSO_4$, 1.8 $\mu$M $FeSO_4$, 55.5 mM glucose, pH 7.3. The medium was supplemented with 1 g of $(^{15}NH_4)_2SO_4$.

*NMR Spectroscopy and Structure Calculation*—One-mg samples of unlabeled TM IV peptide were prepared in $CD_3OH$; trifluoroethanol: $H_2O$ mixtures; $CD_3OH$:$CDCl_3$:$H_2O$ (4:4:1 v/v/v); and $Me_2SO$. Note that for $CD_3OH$:$CDCl_3$:$H_2O$, screw-cap NMR tubes (535-TR-7, Wilmad Labglass, Buena, NJ) were used to prevent solvent evaporation. Chemical shifts were referenced internally to DSS at 0.5 mM, with indirect referencing employed for $^{15}N$ (16). One-dimensional $^1H$ NMR spectra were acquired at 500 MHz on a Varian INOVA spectrometer at a variety of temperatures for each solvent.

Samples for extended analysis were prepared in $Me_2SO$ and in $CD_3OH$:$CDCl_3$:$H_2O$ (4:4:1 v/v/v) at ~2 mM peptide and 1.0 mM DSS. One-dimensional $^1H$, natural abundance $^{15}N$ HSQC, TOCSY (60-ms

mix; DIPSI spin lock), and NOESY (150-ms mix) experiments were acquired on the NANUC Varian INOVA 800 MHz spectrometer for each sample. Double-quantum filtered correlation spectroscopy and NOESY spectra at various mixing times were acquired at 600 MHz on either Varian UNITY or INOVA spectrometers. By using uniformly $^{15}N$-labeled peptide, the three-dimensional $^{15}N$-edited NOESY-HSQC (150-ms mixture), TOCSY-HSQC (57-ms mixture, DIPSI spin lock), and HNHA experiments were acquired at 500 MHz on a Varian Inova spectrometer. Spectra were processed either using VNMR (Varian Inc., Palo Alto, CA) or NMRPipe (17); spectral analysis was facilitated with Sparky 3 (T. D. Goddard and D. G. Kneller, University of California, San Francisco).

Structure calculation was carried out in CNS version 1.1 (18) using NOE contacts derived from the 150-ms mixing time experiments at 800 MHz and $^3J$-coupling constants derived from the HNHA experiments at 500 MHz as described by Vuister and Bax (19). Homonuclear NOESY and HNHA peaks were manually picked in Sparky, and volumes were calculated using Gaussian fits, with motion of the peak center generally allowed; in some cases (<2%) with the NOESY spectra, Sparky's gaussian fit algorithm did not find a convergent solution, and a summed signal intensity was used instead over a manually specified region. Initial NOE calibration was carried out empirically from peak volumes to provide a value in the range of 1.8–5.0 Å. These estimates were used to bin each contact into one of strong (1.8–2.8 Å), medium (1.8–3.6 Å), or weak (1.8–5.0 Å). Peaks with an ambiguous assignment between two possible contacts were assigned to the more conservative contact (where possible) as a starting point.

An iterative procedure was employed to refine and prune the NOE contacts using a philosophy similar to that of Wang *et al.* (20). Families of 500–1000 structures were generated by simulated annealing using the default CNS heating and cooling cycles and NOE energetics. NOE violations were analyzed over each ensemble, and any violations observed in more than ~10% of the ensemble structures were examined in detail. If unambiguous, these were typically lengthened, and if ambiguous, they were reassigned or discarded. During this process, restraints were extended to a fourth "very weak" category (1.8–6.0 Å) as necessary (20). After all major NOE violations were resolved, the three-bond $J$-coupling values were incorporated directly into the simulated annealing protocol (21) using Karplus coefficients as specified by Vuister and Bax (19) for the HNHA experiment for the more structured $CD_3OH$:$CDCl_3$:$H_2O$ condition. A further pair of iterations was carried out to optimize the compatibility between $^3J$-coupling values and NOE restraints. The homoserine lactone residue was incorporated into structure calculations using a protonated residue structure attached to an N-terminal methyl ketone group calculated by MM+ molecular mechanics with bond dipole electrostatics with atomic charges obtained by Restricted Hartree-Fock calculation in HyperChem 3 (Hypercube, Gainesville, FL). XPLO2D 3.2.2 (22) was used to produce CNS topology and parameter files. Structurally convergent segments of the peptide were determined by examining the lowest energy 600 structures out of the final ensemble of 1000 with NMRCORE 1.0 (23); structural features of the 600-member ensemble were analyzed using PROMOTIF-NMR 3.0 (24). The final sets of restraints have been deposited in the Protein Data Bank (entry 1Y4E) along with the 100 lowest energy structures for the $CD_3OH$:$CDCl_3$:$H_2O$ solvent condition.

## RESULTS

*Activity and Expression of NHE1 Mutants*—Fig. 1 illustrates a general model of the $Na^+/H^+$ exchanger (Fig. 1*A*) and a schematic model illustrating TM IV (Fig. 1*B*). To examine which amino acids of TM IV were critical for the activity of the $Na^+/H^+$ exchanger and which amino acids were pore-lining, we used the cysteine-less $Na^+/H^+$ exchanger (cNHE). Each residue in TM IV of cNHE1 was individually mutated to a cysteine residue. Initial experiments examined whether these mutant forms of the $Na^+/H^+$ exchanger had activity. Most surprisingly, TM IV was exquisitely sensitive to mutation. Fig. 2 shows the effects of mutation of amino acids of TM IV to cysteine on NHE activity. Substitution of any of the amino acids with cysteine in TM IV resulted in significant reductions of the measurable activity of the protein in all mutants ($p < 0.05$). In particular, residues $Phe^{155}$, $Leu^{156}$, $Ser^{158}$, $Asp^{159}$, $Phe^{162}$, $Phe^{164}$, $Pro^{167}$, $Pro^{168}$, $Asp^{172}$, $Tyr^{175}$, and $Phe^{176}$ retained less than 20% of the control activity. These mutants were not used for further characterization of activity. We have demonstrated previously that $Pro^{178}$ is not critical for function of NHE1 (10).

Fig. 3 illustrates a Western blot of total cell extracts from AP1 cells stably expressing the single cysteine mutants. Both the mutant and wild-type exchangers displayed the same pattern of immunoreactive bands, with a larger band at ~110 kDa that represents the glycosylated form of the mature $Na^+/H^+$ exchanger and a smaller band at ~95 kDa that represents an immature form of the exchanger that is not fully glycosylated (10). Both the native wild-type NHE and the cysteine-less NHE1 showed strong immunoreactive bands of 110 kDa size and a weaker 95-kDa, unglycosylated NHE1. The amount of mature 110-kDa NHE is quantified below each lane in Fig. 3, relative to cNHE1. Cells lines containing the mutants F155C, Q157C, L163C, L166C, I170C, A173C, G174C, Y175C, L177C and possibly S158C and F176C have relatively normal levels of expression. Several cell lines expressed mainly or a high proportion of the 95-kDa form of the protein, including L156C, D159C, F161C, F162C, P167C, P168C, I169C, L171C, Y175C, and F176C. Several cell lines also expressed much less of the mature protein. These mutants included L156C, D159C, V160C, F161C, F162C, F164C, L165C, P167C, P168C, I169C, L171C, and D172C.

We examined the sensitivity to MTSET or MTSES of the mutant $Na^+/H^+$ exchangers that had greater than 20% residual activity of the cysteine-less NHE1 (Fig. 4). Of the active $Na^+/H^+$ exchangers, only F161C was affected by treatment with either MTSET or MTSES. This resulted in decreases in $Na^+/H^+$ exchanger activity of ~60 and 80%, respectively. To

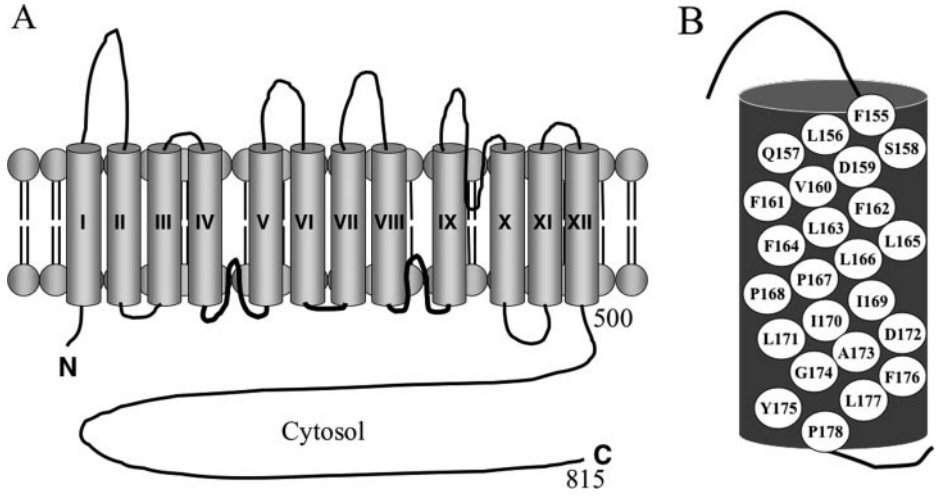


FIG. 1. *A*, topological model of the NHE1 isoform of the $Na^+H^+$ exchanger. The orientation of TM segments I–XII of the NHE1 isoform of the $Na^+/H^+$ exchanger is illustrated (6). *B*, crude model of amino acids present in TM IV.

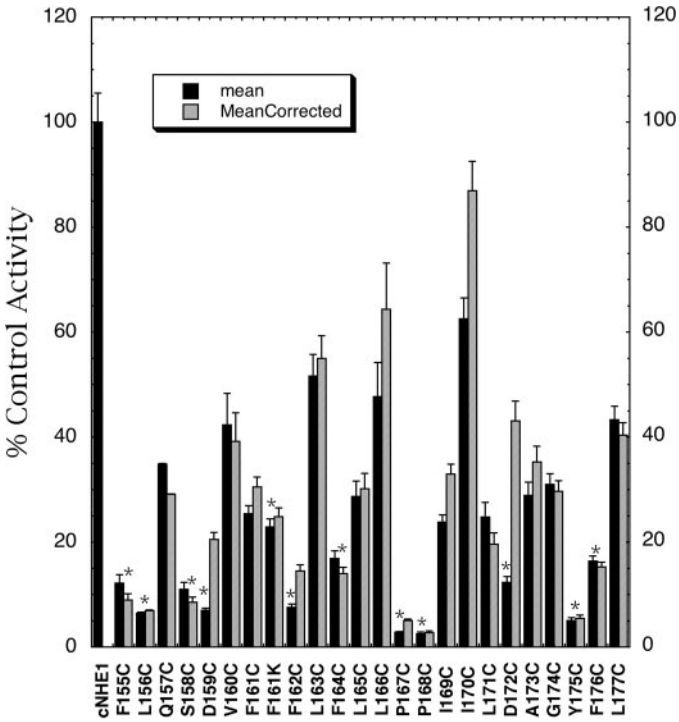


FIG. 2. **Rate of recovery from an acid load by AP-1 cells stably transfected with cNHE1, and $Na^+/H^+$ exchanger mutants (Phe[155] to Leu[177] individually changed to Cys plus F161K).** $Na^+/H^+$ exchanger activity was measured after transient induction with an acid load as described under "Experimental Procedures." The activity of cNHE1 stably transfected with NHE1 was 3.2 pH units/min, and this value was set to 100%. All mutations to cysteine were done in the background of the cysteine-less NHE1, and activities are percent of those of cNHE. The F161K mutation was done in the wild-type NHE1 background, and its activity is expressed as a percent of the wild-type NHE1 activity (4.25 pH units/min). All results are means ± S.E. of at least 10 determinations from two independently made stable cell lines. Results are shown for mean activity both uncorrected (*black*) and normalized for surface processing (*hatched*). * indicates mutants with unnormalized activity that is less than 20% of cNHE1.

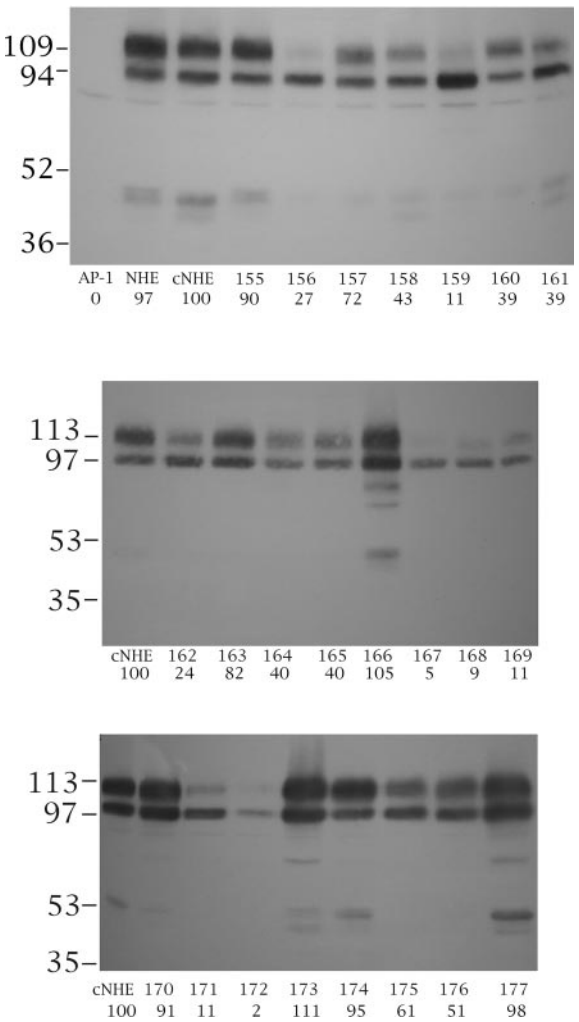


FIG. 3. **Western blot analysis of cell extracts from control and stably transfected AP-1 cells.** Cell extracts were prepared from control (*AP-1*) cells and from cells stably transfected with cDNA coding for HA-tagged cells: wild-type NHE1 (*NHE*), cysteine-less NHE1 (*cNHE*), F155C, L156C, Q157C, S158C, D159C, V160C, F161C, F162C, L163C, F164C, L165C, L166C, P167C, P168C, I169C, I170C, L171C, D172C, A173C, G174C, Y175C, F176C, and L177C. 100 $\mu$g of total protein was loaded in each lane. Results are typical of at least two experiments. *Numbers* below the lanes indicate the values obtained from densitometric scans of the 110-kDa band relative to cNHE1.

confirm that Phe[161] was a critical residue, we created the mutant F161K, which introduced a positive charge into this location in the wild-type NHE1 background. This mutant retained only ~23% of wild-type NHE activity (Fig. 2), had reduced expression (not shown), and reduced surface processing (Table I) relative to wild-type NHE1 supporting the importance of Phe[161] in NHE1 function.

*Subcellular Localization of the Mutant and Wild-type $Na^+/H^+$ Exchangers*—We have earlier found that mutation of amino acids of the $Na^+/H^+$ exchanger sometimes causes the protein to be targeted to an intracellular location (10, 25). We therefore used quantitative measurement of the intracellular localization of NHE1 within AP-1 cells. Cells were treated with sulfo-NHS-SS-biotin and then lysed and solubilized, and labeled proteins were bound to streptavidin-agarose beads. An equal amount of the total cell lysate and unbound lysate was separated by size using SDS-PAGE followed by Western blotting with anti-HA antibody to identify tagged NHE1 protein. Fig. 5 illustrates examples of the results, and Table I summarizes the results quantitatively. In Fig. 5, the total lanes (*T*) and intracellular lanes (*I*) illustrate the NHE1 protein present in these samples. The intracellular lane I was that fraction of the $Na^+/H^+$ exchanger that did not bind to the streptavidin-agarose beads. Cysteine-less NHE1 and most of the mutant exchanger proteins were predominantly present on the plasma membrane in similar amounts. $Na^+/H^+$ exchanger mutants D159C and D172C were significantly reduced in expression on the plasma membrane of the cell. Correcting the activity of these mutants for changes in targeting (Fig. 2) demonstrated that a significant amount of the apparent reduction in activity was because of mistargeting of these proteins. Nevertheless, both still retained less than half of the activity of the cysteine-less NHE1 protein. Correcting for targeting did not greatly change the values for activity of other mutants with the next largest changes being increases in activity of about 20% for L166C and I170C proteins.

*Production and Characterization of TM IV*—To examine the structure of TM IV, we produced it as a fusion protein with GB1. On SDS-PAGE, the fusion protein appeared as a band of ~8 kDa in size (not shown). This was slightly less than the predicted size of 11 kDa. We confirmed the identity of the protein by mass spectrometry, suggesting that the protein ran with a somewhat anomalous weight, typical of many membrane proteins. The yield of the GB1-TM IV fusion protein was typically ~25 mg/liter of cells. After CNBr treatment to free TM IV, it was then purified by reverse phase HPLC. We confirmed the identity of TM IV by mass spectroscopy. For the unlabeled TM4, the expected mass (with a C-terminal homo-

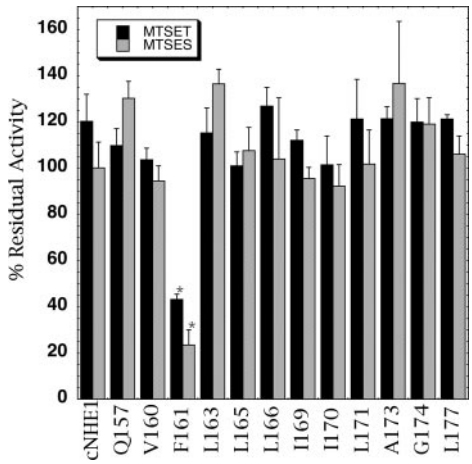


FIG. 4. **Effect of MTSET and MTSES on activity of cNHE1 and single cysteine mutant NHE1 containing cell lines.** $Na^+/H^+$ exchanger activity was measured after transient induction with an acid load as described under "Experimental Procedures." Cells were subsequently treated with 10 mM reagent before a second transient acidification. Results illustrated represent the % of activity after the second acid load, in comparison to the first. * indicates that the second recovery from acid load was significantly lower than the first at $p < 0.01$, Mann-Whitney *U* test. *Solid filled bars* represent MTSET treatments, and *hatched bars* represent MTSES treatments.

TABLE I

*Summary of subcellular localization in AP-1 cells of wild type (wNHE1), cysteine-less NHE1 (cNHE1), and TM IV $Na^+/H^+$ exchanger mutants*

Analysis of localization was as described under "Experimental Procedures." The percent of the total NHE1 protein that was found within the plasma membrane is indicated. The results are mean ± S.E. of at least three determinations.

| Cell line | Plasma membrane |
|---|---|
| | *% total* |
| WNHE1 | 76.9 ± 5.2 |
| CNHE1 | 50.6 ± 6.8 |
| F155C | 68.9 ± 5.4 |
| L156C | 47.5 ± 1.4 |
| Q157C | 60.6 ± 2.0 |
| S158C | 65.3 ± 2.2 |
| D159C | 17.3 ± 3.8[a] |
| V160C | 54.6 ± 3.6 |
| F161C | 42.2 ± 2.5 |
| F161K | 46.6 ± 6.4[a,b] |
| F162C | 26.5 ± 8.2 |
| L163C | 47.5 ± 4.6 |
| F164C | 61.1 ± 0.8 |
| L165C | 48.2 ± 9.4 |
| L166C | 37.5 ± 3.9 |
| P167C | 28.2 ± 9.9 |
| P168C | 47.3 ± 5.3 |
| I169C | 36.6 ± 7.1 |
| I170C | 36.4 ± 2.0 |
| L171C | 64.1 ± 4.2 |
| D172C | 14.5 ± 1.3[a] |
| A173C | 41.5 ± 5.6 |
| G174C | 52.8 ± 10.2 |
| Y175C | 46.8 ± 2.2 |
| F176C | 54.4 ± 3.9 |
| L177C | 54.3 ± 7.3 |

[a] Values indicate significantly reduced in comparison to cNHE1 at $p < 0.05$.

[b] Values indicate significantly reduced in comparison to wNHE1 at $p < 0.05$.

serine lactone) is 3138.8 atomic mass units, and the observed mass in retained preparative HPLC fractions ranged over 3138.4–3134.0 atomic mass units (parent peak mass differed slightly from fraction to fraction; ionic adducts also observed). Impurities at 4405–4411 and 9910–9915 atomic mass units

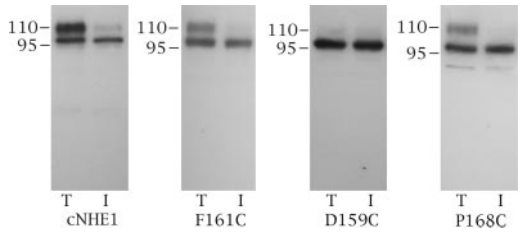


FIG. 5. **Example of a Western blot for determination of localization of the $Na^+/H^+$ exchanger.** Sulfo-NHS-SS-biotin-treated cells were lysed, and solubilized proteins were treated with streptavidin-agarose beads to bind labeled proteins as described under "Experimental Procedures." Equivalent samples of total cell lysate (*T*) and unbound lysate (*I*, intracellular) were run on SDS-PAGE. Western blotting with anti-HA antibody identified NHE1 protein. *cNHE1*, cysteine-less NHE1; representative mutants are F161C, D159C, and P168C.

were detected in less than 25% of the total pooled fractions each, at intensities ranging from 0.5 to 2% relative to the parent peak plus ionic adducts. For the uniformly $^{15}N$-labeled peptide, the expected mass was 3165.8, and observed mass range was 3165.6–3171.6 atomic mass units. Impurities at mass 3085–3086, 4428–4430, and 4816–4820 atomic mass units were detected in less than 10% of the total pooled fractions each, at intensities ranging from 1 to 4% relative to the parent peak plus ionic adducts. Purity was therefore estimated to be greater than 95% for each of the peptides after pooling of the HPLC fractions.

*Choice of NMR Conditions*—To determine the structure of TM IV, we tested several solvent mixtures. The trifluoroethanol:$H_2O$ mixtures and methanol appeared more promising than either the $CD_3OH$:$CDCl_3$:$H_2O$ mixture or $Me_2SO$, in that wider dispersions of chemical shifts were observed in the backbone $H^N$ (7–9 ppm) and $H^\alpha$ (3.5–5 ppm) regions of one-dimensional $^1H$ spectra (data not shown). Unfortunately, the peptide precipitated out of each of these solutions within days, making multidimensional NMR data acquisition impractical. In the range of 5–40 °C, 30 °C gave rise to well resolved, minimally broadened $^1H$ spectra (data not shown). Therefore, structural studies were carried out in $CD_3OH$:$CDCl_3$:$H_2O$ and $Me_2SO$ at 30 °C. These ~2 mM peptide samples with 0.5 mM DSS as the internal chemical shift reference are stable at room temperature, providing reproducible spectra over the course of several months.

*Resonance Assignment*—Standard sequential assignment methods were applied (26), using TOCSY and double-quantum filtered correlation spectroscopy experiments along with $H^N$ values observed by natural abundance $^{15}N$-HSQC experiments for spin-system assignment and NOESY connectivity data to walk through the sequence. This provided assignment of all backbone $H^N$ and $H^\alpha$, except for the N-terminal $H^N$, all side chain $H^\beta$ resonances, and most other side chain proton resonances. The C-terminal residue was identified as a homoserine lactone rather than free homoserine, because its $H^\alpha$ and side chain $^1H$ chemical shifts correspond to $\alpha$-amino-$\gamma$-butyrolactone rather than to L-homoserine (27). This was upheld by the molecular weight indicated by MALDI-MS of the purified peptide when considering the fact that homoserine lactone residues are not subsequently undergoing conversion to the free homoserine moiety, because this reaction is reported to be very slow at the peptide C terminus even with catalytic basic conditions (28). Due to spectral overlap even at 800 MHz, caused primarily by repetition in the primary sequence, a few side chain protons could not be resolved. In $CD_3OH$:$CDCl_3$:$H_2O$, aromatic ring protons could not be identified, and $H^\delta$ shifts for residues $Leu^{165}$, $Pro^{167}$, $Ile^{169}$, $Pro^{178}$, and $Leu^{179}$, and $H^\gamma$ of $Pro^{167}$ were unresolved. In $Me_2SO$, all aliphatic side chain resonances were resolved, and all ring $H^\delta$ resonances; in the

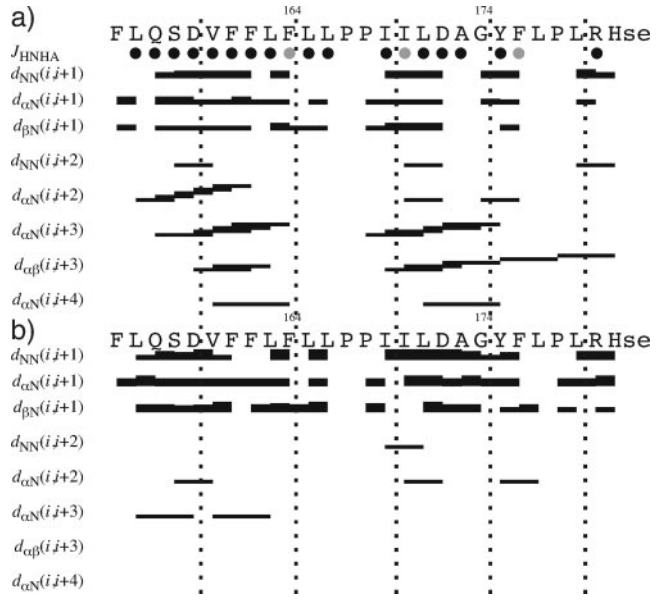


FIG. 6. **Summary of NOE connectivities (150 ms mixing time) observed between the indicated pairs of $H^N$, $H^\alpha$, and $H^\beta$ protons of the TM4 segment in $CD_3OH$:$CDCl_3$:$H_2O$ (4:4:1 v/v/v) (*a*) and $Me_2SO$ (*b*).** *Dashed lines* separate groups of five residues. Residues for which $J_{HNHA}$ values were usable in $CD_3OH$:$CDCl_3$:$H_2O$ are indicated by *circles colored black* for ±2-Hz restraints or *gray* for ±2.5-Hz restraints. Figure modified from CYANA (L. A. Systems Inc.) output.

case of $Phe^{155}$ and $Tyr^{175}$, $H^\epsilon$ resonances were also resolved. Note that frequent overlap of $H^\beta$ and $H^\gamma$ resonances was observed with Leu and Ile side chains. $^{15}N$-Edited TOCSY and NOESY experiments with uniformly labeled peptide samples confirmed spin system and resonance assignment and allowed several additional protons to be assigned. Finally, natural abundance $^{13}C$-HSQC experiments allowed identification of all $C^\alpha$ and $C^\beta$ resonances except $C^\alpha$ of the C-terminal homoserine lactone in $CD_3OH$:$CDCl_3$:$H_2O$ and $C^\beta$ of $Pro^{167}$ in $Me_2SO$ All resonance assignments have been deposited in the BioMagResBank.

*Structure Calculation*—Homonuclear NOESY experiments were used exclusively to define NOE contacts between protons. A variety of mixing times was examined under each solvent condition (100–450 ms; data not shown). In each of the solvents, the 150-ms mixing time provided peaks of sufficient intensity to analyze without apparently extensive spin diffusion. Therefore, this mixing time was employed for quantitative peak volume analysis. A large number of intra- and inter-residue contacts were observed in each solvent condition. In $Me_2SO$, 302 intra-molecular, 244 sequential, and 62 medium range contacts were unambiguously assigned. In $CD_3OH$:$CDCl_3$:$H_2O$, there were 222 intra-residue, 140 sequential, and 96 medium range unambiguous contacts assigned. More contacts were able to be assigned in the $Me_2SO$ conditions due to the additional Phe and Tyr ring proton assignments. In $CD_3OH$:$CDCl_3$:$H_2O$, the TM IV sample showed two regions with significant $i,i+3$ contacts, often indicative of $\alpha$-helical character, which were not apparent in $Me_2SO$ (Fig. 6). The first of these regions is coincident with a large number of $i,i+2$ contacts, however, which together indicate potential $\beta$-turns. Chemical shifts have not at present been incorporated into the structural calculations because a quantitative comparison to random coil or BioMagResBank average chemical shifts observed in aqueous solution may be altogether incorrect. $^3J$-coupling constants extracted from $^{15}N$-edited HNHA experiments were used where possible to aid in specifying $\phi$-dihedral angles during the simulated annealing protocol. Because the peptide was less structured in $Me_2SO$ than in $CD_3OH$:$CDCl_3$:$H_2O$, as evinced by the greatly reduced number of medium range NOE contacts (Fig. 6), we analyzed in detail only the $CD_3OH$:$CDCl_3$:$H_2O$ structural features present. The characteristics of the final ensemble of retained structures are given in Table II.

TABLE II
*Structural statistics for the final ensemble of 600 structures out of the 1000 calculated for $CD_3OH$:$CDCl_3$:$H_2O$*

| Nonredundant NOE restraints | |
|---|---|
| Total | 458 |
| Intra-residue | 222 |
| Sequential | 140 |
| Medium range ($\|i-j\| \leq 4$) | 96 |
| Energies (kcal/mol) | |
| $E_{Total}$ | 106.8 ± 9.8 |
| $E_{NOE}$ | 8.67 ± 2.04 |
| Restraint violations | |
| 0.3 Å > \|NOE − distance\| > 0.2 Å | 12 |
| \|NOE − distance\| ≥ 0.3 Å | 0 |
| $J_{HNHA}$ violations | 81 |

## DISCUSSION

*Functional Analysis of TM IV*—Transmembrane segment four (TM IV; residues 155–177) of the NHE1 isoform of the $Na^+/H^+$ exchanger has been implicated in the ion transport and inhibitor binding properties of the protein (7–9). We have recently shown (10) that the double proline pair $Pro^{167}$ and $Pro^{168}$ is critical for the function of NHE1. They were suggested to be critical in the maintenance of an appropriate structure of TM IV and necessary for normal NHE1 transport function. One method to determine the functional role of individual amino acids of a transmembrane segment of a membrane protein is cysteine-scanning mutagenesis in combination with reaction with sulfhydryl reagents. Cysteine-scanning mutagenesis takes advantage of the fact that the sulfhydryl moiety is the most reactive functional group in a protein (29). It has been used to determine pore-lining residues in numerous membrane proteins (30–32), including the lactose permease of *E. coli* (33), the mouse acetylcholine receptor (34), the human glucose transporter Glut1, and the human anion exchanger isoform 1 (AE1) (35). Cysteine-scanning mutagenesis uses the highly reactive sulfhydryl moiety to determine the accessibility of side chains of amino acids. Two sulfhydryl-reactive reagents (36) that are often used in these studies are MTSET and MTSES, which are membrane-impermeant (37, 38), react with pore-lining residues surrounded by water, and cannot reach residues within the hydrophobic bilayer.

Initial experiments substituted each of the amino acids in TM IV of cysteine-less NHE1 with cysteine residues. We found that TM IV was exquisitely sensitive to mutation. Twelve of the cysteine mutants had less than 20% of the activity of the control cNHE1. Western blotting revealed that in some cases the reduction in activity was due to a lower level of expression of the protein (Fig. 3); however, in most cases correction for the amount of plasma membrane protein (Table I and Fig. 2) did not explain the loss of activity. Several of the mutants were expressed mainly as unglycosylated protein, and many but not all of these had greatly reduced activity. We have found previously that mutation of some amino acids can greatly affect the glycosylation levels of the proteins. We examined if these mutations affected the surface targeting of the protein. Our findings that many of the mutations of TM IV affected targeting, expression, or activity are similar to the results found with the human anion exchanger (35) and with TM XI of lactose permease (33). In contrast, for the tetracycline-resistant transporter of *E. coli* (39) and in P-glycoprotein (40), it was possible

to mutate all the amino acids of a TM segment and always retain appreciable activity. This susceptibility to mutation appears to vary not only between proteins but also within different transmembrane segments of the same protein. TM XI of lactose permease had several sensitive amino acids (33), whereas TM XII only had one (41). This property could be reflective of both the importance of the residues in the particular segment, and of the importance of the segment itself to the structure and function of the protein. In our case, it was clear that there was a relatively strict requirement for many of the amino acids of TM IV, and this could be indicative of precise structural and functional roles.

Treatment with both positively charged MTSET and negatively charged MTSES revealed that $Phe^{161}$ is accessible to and reacts with these sulfhydryl-reactive reagents (Fig. 4). The most likely explanation for this reactivity is an interaction at a site that lines the ion translocation pore. The reagents then at least partially block the pore and inhibit ion transport (35). Thus, $Phe^{161}$ in TM IV is the first residue to be unambiguously identified as lining the ion transport pore of NHE1. Mutation of $Phe^{161}$ to Lys resulted in loss of most of NHE1 activity (Fig. 2), confirming that this is a critical amino acid.

*Structural Analysis of TM IV*—We examined the structure of TM IV in $CD_3OH$:$CDCl_3$:$H_2O$ and in $Me_2SO$ at 30 °C. As with many peptides studied by NMR (20, 42) the TM IV segment does not, as a whole, assume a single conformation. Rather, sections within the peptide converge structurally. Consideration of these sections relative to each other then provides insight into the TM IV segment overall. In a given state of the intact NHE1 protein, a single conformation would presumably be preferred by the TM IV segment. However, the structures that we present here represent the most energetically favorable forms of this TM segment in a low dielectric environment mimicking both a lipid bilayer and a protein interior. Therefore, it is reasonable to presume that they would also be favorable within the setting of the NHE1 protein. Indeed, a number of studies have demonstrated strong correspondence between structures of peptides or protein segments obtained in membrane mimetic solvents to structures obtained by solution state NMR in micelles or to entire membrane proteins determined by x-ray crystallography (11–13). Most interestingly, we find that $CD_3OH$:$CDCl_3$:$H_2O$ provides a well defined peptide structure, whereas the peptide in $Me_2SO$ appears much less structured. This implies that there is a great deal of value in determining membrane peptide structures in multiple solvent conditions, because a single solvent may not induce sufficient sampling of the structured state.

Three sections of four to nine residues of the TM IV segment converge structurally and were defined as core regions by NMRCORE (23) and confirmed by analysis of r.m.s.d. values (Table III). Namely, the stretches of residues $Asp^{159}$–$Leu^{163}$, $Leu^{165}$–$Pro^{168}$, and $Ile^{169}$–$Phe^{176}$ each converge. These are illustrated in Fig. 7 (*a–c*), and their relationship is demonstrated schematically in Fig. 7*d*. Each section superposes extremely well, with all convergent residues identified in Fig. 7*d* for the 600-member ensemble having a $C^\alpha$ r.m.s.d. relative to the average structure in the range of 0.25–0.85 Å. The heavy backbone and side chain atom r.m.s.d. are <1.5 Å over $Asp^{159}$–$Leu^{163}$ and $Ile^{169}$–$Gly^{174}$ as well as for $Leu^{165}$ and $Pro^{167}$ (Table III), which implies good structural convergence at the side chain level for these segments. The boundary points of converged stretches are also very clear upon examination of the r.m.s.d. values in Table III as follows: $Ser^{158}$ and $Gln^{157}$ rapidly diverge from $Asp^{159}$–$Leu^{163}$; $Phe^{164}$ has a much higher r.m.s.d. than the surrounding residues when the peptide structures are superposed at either 159–163 or 165–168; $Pro^{168}$ clearly fits well with 165–168 but not with 169–176, whereas the converse is true of $Ile^{169}$; finally, $Leu^{177}$, $Pro^{178}$, and $Leu^{179}$ demonstrate large jumps in r.m.s.d. values relative to the superposition 170–178. One of the ensemble members is shown in Fig. 7*e* as a representative structure. Given that the segment must span a membrane with the width on the order of 25–35 Å, a relatively extended ensemble member such as that pictured in Fig. 7*e* is more representative of the expected biological configuration than one that curls back upon itself. This particular structure must be considered as only demonstrative of the relation between the convergent segments of the TM IV segment, rather than as representative of any global structuring.

TABLE III
*r.m.s.d. for $C^\alpha$ and for all heavy atoms of the 600 lowest energy structures of the 1000-member ensemble of the TM IV peptide superposed over each convergent stretch and given relative to the average structure for that superposition*

Residues outside converged segments and at borders between convergent segments are also shown.

| Residue | r.m.s.d., $C^\alpha$ | r.m.s.d., all heavy atoms |
|---|---|---|
| $Gln^{157}$ [a,b] | 1.83 | 3.43 |
| $Ser^{158}$ [a,b] | 1.23 | 1.86 |
| $Asp^{159}$ [a] | 0.43 | 1.24 |
| $Val^{160}$ [a] | 0.25 | 0.59 |
| $Phe^{161}$ [a] | 0.30 | 1.42 |
| $Phe^{162}$ [a,b] | 0.45 | 1.50 |
| $Leu^{163}$ [a] | 0.53 | 1.16 |
| $Phe^{164}$ | 1.54[a]/2.49[c] | 2.65[a]/4.00[c] |
| $Leu^{165}$ [c] | 0.80 | 1.40 |
| $Leu^{166}$ [c] | 0.57 | 1.94 |
| $Pro^{167}$ [c] | 0.38 | 0.85 |
| $Pro^{168}$ | 0.85[c]/1.43[d] | 1.55[c]/1.81[d] |
| $Ile^{169}$ [b] | 3.16[c]/0.76[d] | 4.36[c]/1.34[d] |
| $Ile^{170}$ [d] | 0.70 | 1.24 |
| $Leu^{171}$ [d] | 0.59 | 1.41 |
| $Asp^{172}$ [d] | 0.48 | 1.32 |
| $Ala^{173}$ [d] | 0.52 | 0.64 |
| $Gly^{174}$ [b,d] | 0.55 | 0.56 |
| $Tyr^{175}$ [d] | 0.36 | 2.00 |
| $Phe^{176}$ [d] | 0.70 | 1.77 |
| $Leu^{177}$ [b,d] | 1.24 | 2.61 |
| $Pro^{178}$ [d] | 1.36 | 1.64 |
| $Leu^{179}$ [b,d] | 2.66 | 3.53 |

[a] Superposed on $C^\alpha$ of 159–161 and 163 using LSQKAB (50, 51).
[b] Not defined as core using program NMRCORE.
[c] Superposed on $C^\alpha$ of 165–168.
[d] Superposed on $C^\alpha$ of 170–173, 175–176, and 178.

The first feature of note is that the TM IV segment certainly does not resemble a canonical transmembrane $\alpha$-helix. This is despite the fact that there are helix-capping sequences inherent within the TM IV over the segment studied. The N-terminal sequence FLQSDV (155–160) fits well with a type Ib cap, whereas the sequence LDAGYF (171–176) fits a type Va C-terminal cap, with capping nomenclature as defined by Aurora and Rose (43). These cap sequences would imply that a helix should form between $Leu^{156}$ and $Asp^{173}$. However, the NMR data readily demonstrate a lack of helicity, even at relatively long NOESY mixing times. Contiguous $i,i+3$ and $i,i+4$ contacts indicative of an $\alpha$-helix (26) are not observed. In fact, as implied in Fig. 7*d,* only a very short stretch of the segment even approaches a helical structure. This should not be taken to imply a lack of structure; in fact, eight type IV $\beta$-turns occur in a major proportion of ensemble members, with four found in more than 90% of the structures. Note that this means a frequent observance of "disallowed" $\phi/\psi$ angles would actually be expected (44), and correspondingly, a PROCHECK-NMR (45) analysis places 12.2% of the non-Pro and Gly residues in the disallowed region of the Ramachandran plot.

Of the three core regions defined by convergent backbone atoms, residues $Asp^{159}$–$Leu^{163}$ are the most affected by these

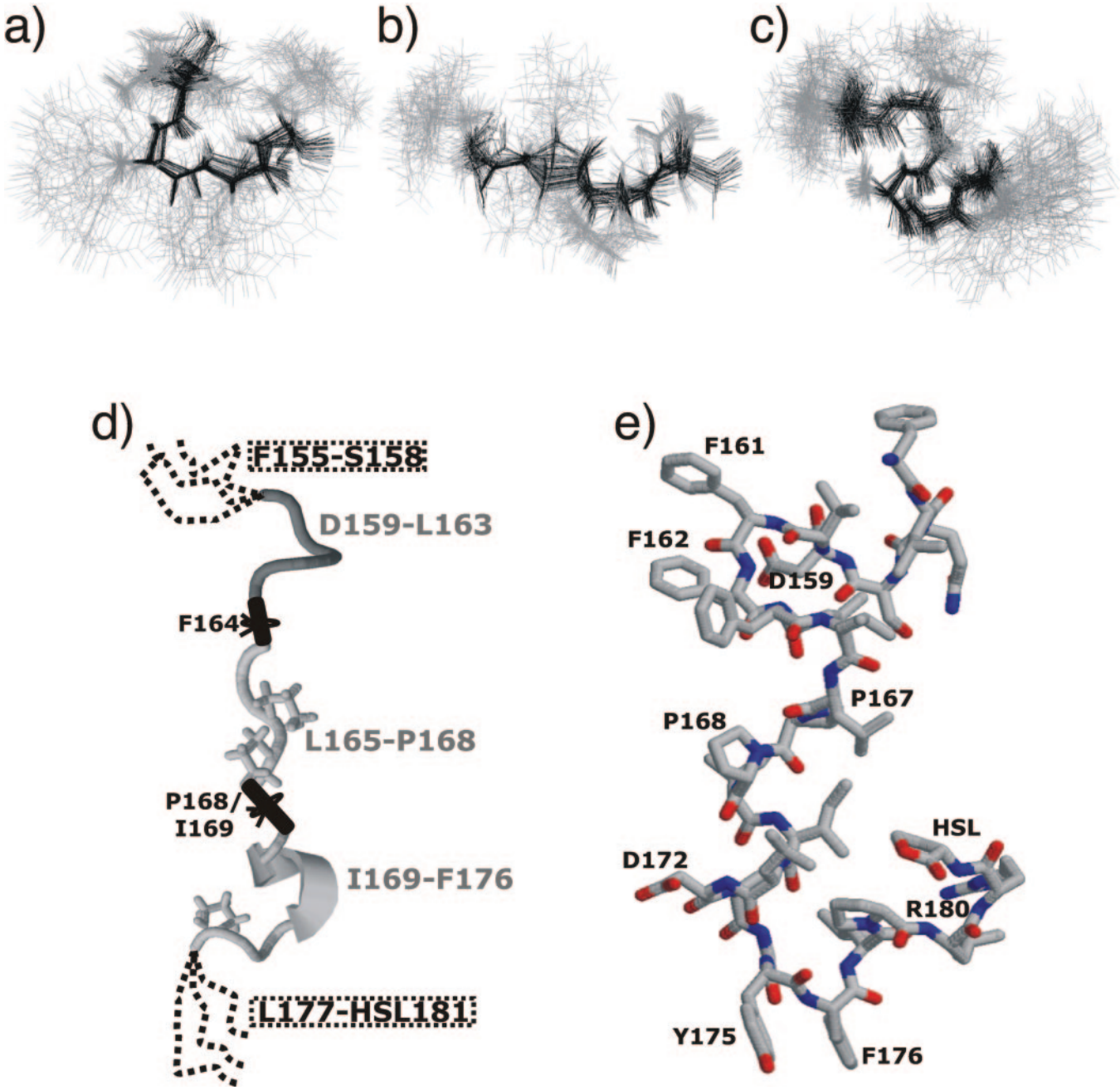


FIG. 7. **Convergent structural motifs pinpointed by NMRCORE (23) in the lowest energy 600 members of the final 1000 structure ensemble satisfying NOE and *J*-coupling restraints determined for the TM4 peptide in $CD_3OH$:$CDCl_3$:$H_2O$ (4:4:1 v/v/v).** *a–c* show the lowest energy 60 structures, with backbone atoms colored *black* and side chains *gray*. *a,* convergent loop structure over residues 159–163; *b,* defined extended structure over 165–168; and *c,* helical stretch at 169–176. *d,* schematic demonstrating convergent stretches (*gray*) in relation to pivot residues $Phe^{164}$ and $Pro^{168}$/$Ile^{169}$ (*black*) and flexible N and C termini (*dashed lines*). Note that only proline side chains are drawn. *e, stick diagram* with Cory, Pauling, Koltun coloring of a single member of the ensemble (*i.e.* the flexible linkers and termini in *d* have assumed a discrete configuration) demonstrating the overall extended nature of the peptide.

$\beta$-turns. $Asp^{159}$ is the $i + 2$ residue in one type IV turn, and the first residue in a second, $Val^{160}$, is the $i + 3$ and $i + 1$ residue for these turns, as well as the first residue in a third turn; following along the sequence, $Phe^{161}$ and $Phe^{162}$ both participate in the turns initiated at $Asp^{159}$ and $Val^{160}$, and $Leu^{163}$ participates as the $i + 3$ residue for $Val^{160}$. Therefore, this series of turns, observed in 81–94% of the ensemble, serves to converge this five-residue stretch. Most interestingly, $Leu^{165}$–$Pro^{168}$ are nowhere near as strongly influenced by $\beta$-turns. Rather, these residues appear to be quite extended (Fig. 7*b*), with $Pro^{168}$ initiating type I or IV $\beta$-turns in ~85% of the ensemble. Finally, residues $Ile^{169}$–$Phe^{176}$ converge strongly, providing the only appreciable $\alpha$-helical character over the entire transmembrane segment. The helical stretch extends over 4–6 residues for ~77% of the ensemble members, starting between $Ile^{169}$ and $Leu^{171}$ and ending at $Gly^{174}$, with each one of these members of the ensemble showing helical character over the four-residue segment of $Leu^{170}$–$Gly^{174}$. The C terminus of this convergent stretch is defined by $Gly^{174}$ and $Tyr^{175}$, each of which act as the first residue for a sequential pair of type IV $\beta$-turns in 92% or more of the ensemble members.

Although similar experimental resolution in NMR studies has been achieved using micelles in aqueous solution (46), such an environment would surround the TM IV peptide with hydrophobic detergent tails. In its natural setting, this segment of the NHE1 protein would contact lipid tail groups, surrounding

polypeptide segments, and a pore region with a relatively high dielectric constant. In the case where a transmembrane segment has a very clearly defined structure, such as a canonical membrane-spanning $\alpha$-helix, the micellar environment serves as an excellent conformational stabilizer. In the micellar state, we would anticipate that the allowed rotations about $Phe^{164}$ and $Pro^{168}/Ile^{169}$ would be greatly reduced. However, this may actually be an artificial constraint upon the peptide structure relative to the solvent setting, which allows increased conformational sampling. We feel that the present structure in a mixture of solvents representing a variety of dielectrics provides a reliable representation of the best structured regions of the TM IV segment. This should be useful in interpretation of future experiments using more complete sections of NHE1, in particular for solid state NMR experiments that are aided by knowledge of the most likely polypeptide backbone configurations (47).

*Correlating Structural and Functional Data*—In light of the structural data, plausible explanations for the loss in activity observed for some of the most severe cysteine-scanning mutants can be advanced. Mutations to P167C and P168C practically abrogate all exchanger activity, and mutations of these prolines to other residues did not allow for a return to a normally functioning $Na^+/H^+$ exchanger (10). Mutation from an imino to a much freer amino acid moiety would readily modify the structural motif observed at this pair of prolines (Fig. 7*b*). Given the loss of activity, it is likely that the extended structural nature of this motif is crucial in NHE1 folding into the functional form. The Y175C mutation also causes almost complete loss in activity. Most interestingly, $Tyr^{175}$ is observed to participate as the second residue in an extremely well converged double ($i,i + 1$) type IV $\beta$-turn, just N-terminal to the aromatic residue $Phe^{176}$. Note that F176C also causes significant loss of activity. Analysis of the torsion angles defined between the $C^{\alpha}$-$C^{\beta}$, -$C^{\gamma}$, and -$C^{\xi}$ vectors of $Tyr^{175}$ and $Phe^{176}$ for the ensemble of 600 structures shows that the aromatic side chain moieties of $Tyr^{175}$ and $Phe^{176}$ have a strong tendency to fall within ~50° of each other relative to the polypeptide backbone over this region of the TM IV segment. Because these are large, hydrophobic side chains, it seems likely that they would be at the interface with neighboring transmembrane segments or protruding into the lipid bilayer rather than directly into the channel environment. Substitution of these aromatic groups with the significantly less bulky, polar cysteine side chain would disrupt these interactions, thereby disrupting the NHE1 structure as a whole, leading to the observed loss in activity. However, the mutated F161C side chain does appear to be pore-exposed, so this is not a certainty.

The mutation F161C allows for reactivity with the sulfhydryl-reactive reagent MTSET that inhibits $Na^+/H^+$ exchanger activity. This implies that residue 161 is facing the NHE1 translocation pore. With this in mind, examination of the structure of the TM IV segment provides a very interesting revelation. $Phe^{161}$ side chain is actually fully exposed when put in the context of residues $Phe^{155}$–$Ile^{169}$ in every member of the ensemble (data not shown). Because rotation of the structurally convergent sections is observed about $Phe^{164}$ (Fig. 7*d*), any further analysis of the two C-terminal domains relative to $Phe^{161}$ would be purely speculative, and it was therefore not possible to determine at this stage which other C-terminal amino acids face the translocation pore. However, the exposed nature of the $Phe^{161}$ side chain at the extracellular end of the segment is demonstrated in all 600 retained ensemble members satisfying the experimental constraints, meaning that the isolated TM IV segment in membrane mimetic solvent assumes a structure consistent with the reactivity observed for the exchanger as a whole. Over the convergent stretch of $Asp^{159}$–$Leu^{163}$ (Fig. 7*a*), the $Asp^{159}$ side chain is uniformly observed on the same face of the peptide. Therefore, it seems likely that the anionic $Asp^{159}$ side chain would also protrude into the pore of the exchanger, allowing it to act in cation coordination during translocation. Mutation of this amino acid eliminated activity and reduced expression of the protein, consistent with a critical role for this amino acid. We have previously postulated that polar residues within transmembrane segments of the $Na^+/H^+$ exchanger are important in cation coordination and transport (48, 49), and the structure of TM IV supports such a role for this polar residue.

Our study has given the first detailed structural and functional information on TM IV of the NHE1 isoform of the $Na^+/H^+$ exchanger. TM IV appears to be very sensitive to alterations in its amino acid sequence. We show that although it is a well structured transmembrane segment, its structure is uniquely different from a typical $\alpha$-helix. Possibly this reflects its pivotal role in cation binding and transport. $Phe^{161}$ and possibly $Asp^{159}$ are amino acid residues that protrude into the pore of the channel.

*Acknowledgments*—Protein identification and purification were performed at the Institute for Biomolecular Design, University of Alberta, Edmonton, Alberta, Canada. We thank the Canadian National High Field NMR Centre for their assistance in the collection of the 800-MHz data. Operation of Canadian National High Field NMR Centre is funded by the Canadian Institutes of Health Research, Natural Sciences and Engineering Research Council of Canada, and the University of Alberta. We also thank Jeff Devries and Gerry McQuaid for maintaining the 500- and 600-MHz spectrometers and Dr. T. Burrow of the Department of Chemistry, University of Toronto, for useful discussions.

REFERENCES

1. Orlowski, J., and Grinstein, S. (1997) *J. Biol. Chem.* **272,** 22373–22376
2. Grinstein, S., Rotin, D., and Mason, M. J. (1989) *Biochim. Biophys. Acta* **988,** 73–97
3. Pouyssegur, J., Sardet, C., Franchi, A., L'Allemain, G., and Paris, S. (1984) *Proc. Natl. Acad. Sci. U. S. A.* **81,** 4833–4837
4. Fliegel, L. (2001) *Basic Res. Cardiol.* **96,** 301–305
5. Mentzer, R. M., Jr., Lasley, R. D., Jessel, A., and Karmazyn, M. (2003) *Ann. Thorac. Surg.* **75,** S700–S708
6. Wakabayashi, S., Pang, T., Su, X., and Shigekawa, M. (2000) *J. Biol. Chem.* **275,** 7942–7949
7. Counillon, L., Franchi, A., and Pouyssegur, J. (1993) *Proc. Natl. Acad. Sci. U. S. A.* **90,** 4508–4512
8. Counillon, L., Noel, J., Reithmeier, R. A. F., and Pouyssegur, J. (1997) *Biochemistry* **36,** 2951–2959
9. Touret, N., Poujeol, P., and Counillon, L. (2001) *Biochemistry* **40,** 5095–5101
10. Slepkov, E. R., Chow, S., Lemieux, M. J., and Fliegel, L. (2004) *Biochem. J.* **379,** 31–38
11. Girvin, M. E., Rastogi, V. K., Abildgaard, F., Markley, J. L., and Fillingame, R. H. (1998) *Biochemistry* **37,** 8817–8824
12. Katragadda, M., Alderfer, J. L., and Yeagle, P. L. (2001) *Biophys. J.* **81,** 1029–1036
13. Yeagle, P. L., Choi, G., and Albert, A. D. (2001) *Biochemistry* **40,** 11932–11937
14. Lindhout, D. A., Thiessen, A., Schieve, D., and Sykes, B. D. (2003) *Protein Sci.* **12,** 1786–1791
15. Huth, J. R., Bewley, C. A., Jackson, B. M., Hinnebusch, A. G., Clore, G. M., and Gronenborn, A. M. (1997) *Protein Sci.* **6,** 2359–2364
16. Wishart, D. S., Bigam, C. G., Yao, J., Abildgaard, F., Dyson, H. J., Oldfield, E., Markley, J. L., and Sykes, B. D. (1995) *J. Biomol. NMR* **6,** 135–140
17. Delaglio, F., Grzesiek, S., Vuister, G. W., Zhu, G., Pfeifer, J., and Bax, A. (1995) *J. Biomol. NMR* **6,** 277–293
18. Brunger, A. T., Adams, P. D., Clore, G. M., DeLano, W. L., Gros, P., Grosse-Kunstleve, R. W., Jiang, J. S., Kuszewski, J., Nilges, M., Pannu, N. S., Read, R. J., Rice, L. M., Simonson, T., and Warren, G. L. (1998) *Acta Crystallogr. Sect. D Biol. Crystallogr.* **54,** 905–921
19. Vuister, G. W., and Bax, A. (1993) *J. Am. Chem. Soc.* **115,** 7772–7777
20. Wang, J. J., Hodges, R. S., and Sykes, B. D. (1995) *J. Am. Chem. Soc.* **117,** 8627–8634
21. Garrett, D. S., Kuszewski, J., Hancock, T. J., Lodi, P. J., Vuister, G. W., Gronenborn, A. M., and Clore, G. M. (1994) *J. Magn. Reson.* **104,** 99–103
22. Kleywegt, G. J. (1995) *CCP4/ESF-EACBM Newsletter on Protein Crystallography* **31,** 45–50
23. Kelley, L. A., Gardner, S. P., and Sutcliffe, M. J. (1997) *Protein Eng.* **10,** 737–741
24. Hutchinson, E. G., and Thornton, J. M. (1996) *Protein Sci.* **5,** 212–220
25. Murtazina, B., Booth, B. J., Bullis, B. L., Singh, D. N., and Fliegel, L. (2001) *Eur. J. Biochem.* **268,** 1–13
26. Wuthrich, K. (1986) *NMR of Proteins and Nucleic Acids*, Wiley Interscience, New York
27. Pouchert, C. J. (1983) *The Aldrich Library of NMR Spectra*, 2nd Ed., A4, 450–459, 21, 978–997 Aldrich Chemical Co., Milwaukee, WI
28. Ambler, R. P. (1965) *Biochem. J.* **96,** 32P

29. Mattson, G., Conklin, E., Desai, S., Nielander, G., Savage, M. D., and Morgensen, S. (1993) *Mol. Biol. Rep.* **17,** 167–183
30. Yan, R. T., and Maloney, P. C. (1995) *Proc. Natl. Acad. Sci. U. S. A.* **92,** 5973–5976
31. Slotboom, D. J., Konings, W. N., and Lolkema, J. S. (2001) *J. Biol. Chem.* **276,** 10775–10781
32. Doering, A. E., Nicoll, D. A., Lu, Y., Lu, L., Weiss, J. N., and Philipson, K. D. (1998) *J. Biol. Chem.* **273,** 778–783
33. Dunten, R. L., Sahin-Toth, M., and Kaback, H. R. (1993) *Biochemistry* **32,** 12644–12650
34. Akabas, M. H., Stauffer, D. A., Xu, M., and Karlin, A. (1992) *Science* **258,** 307–310
35. Tang, X.-B., Kovacs, M., Sterling, D., and Casey, J. R. (1999) *J. Biol. Chem.* **274,** 3557–3564
36. Stauffer, D. A., and Karlin, A. (1994) *Biochemistry* **33,** 6840–6849
37. Holmgren, M., Liu, Y., Xu, Y., and Yellen, G. (1996) *Neuropharmacology* **35,** 797–804
38. Liu, J., and Siegelbaum, S. A. (2000) *Neuron* **28,** 899–909
39. Kimura-Someya, T., Iwaki, S., and Yamaguchi, A. (1998) *J. Biol. Chem.* **273,** 32806–32811
40. Loo, T. W., and Clarke, D. M. (1999) *J. Biol. Chem.* **274,** 35388–35392
41. He, M. M., Sun, J., and Kaback, H. R. (1996) *Biochemistry* **35,** 12909–12914
42. Spadaccini, R., and Temussi, P. A. (2001) *Cell. Mol. Life Sci.* **58,** 1572–1582
43. Aurora, R., and Rose, G. D. (1998) *Protein Sci.* **7,** 21–38
44. Hutchinson, E. G., and Thornton, J. M. (1994) *Protein Sci.* **3,** 2207–2216
45. Laskowski, R. A., Rullmannn, J. A., MacArthur, M. W., Kaptein, R., and Thornton, J. M. (1996) *J. Biomol. NMR* **8,** 477–486
46. Henry, G. D., and Sykes, B. D. (1994) *Methods Enzymol.* **239,** 515–535
47. Marassi, F. M. (2002) *Concepts Magn. Reson.* **14,** 212–224
48. Dibrov, P., Young, P. G., and Fliegel, L. (1998) *Biochemistry* **36,** 8282–8288
49. Dibrov, P., and Fliegel, L. (1998) *FEBS Lett.* **424,** 1–5
50. Kabsch, W. (1976) *Acta Crystallogr. Sect. A* **32,** 922–923
51. Collaborative Computational Project, Number 4 (1994) *Acta Crystallogr. Sect. D Biol. Crystallogr.* **50,** 760–763